Degradable Latexes by Nitroxide-Mediated Aqueous Seeded Emulsion Copolymerization using Thionolactones

*Maëlle Lages[1], Noémie Gil[2], Paul Galanopoulo[3], Julie Mougin[1], Catherine Lefay[2], Yohann Guillaneuf[2], Muriel Lansalot[3], Franck D'Agosto[3], Julien Nicolas[1]**

[1] Université Paris-Saclay, CNRS, Institut Galien Paris-Saclay, F-91400 Orsay, France

[2] Aix Marseille Univ., CNRS, Institut de Chimie Radicalaire, UMR 7273, F-13397 Marseille, France

[3] Univ Lyon, Université Claude Bernard Lyon 1, CPE Lyon, CNRS, UMR 5128, Catalysis, Polymerization, Processes and Materials (CP2M), F-69616 Villeurbanne, France

*To whom correspondence should be addressed.

Email: julien.nicolas@universite-paris-saclay.fr

Tel.: +33 1 80 00 60 81

Abstract

Thiocarbonyl addition-ring-opening (TARO) polymerization of thionolactones offers the unique opportunity to incorporate thioester functions into vinyl polymer backbones via a radical mechanism. Recently, successful synthesis of degradable vinyl copolymer latexes based on dibenzo[c,e]oxepane-5-thione (DOT) has been reported by free-radical polymerization (FRP) in emulsion and aqueous polymerization-induced self-assembly (PISA). Herein, to combine a controlled radical polymerization process with the avoidance of preliminary synthesis, we performed the aqueous nitroxide-mediated copolymerization (NMP) of DOT and *n*-butyl acrylate (*n*BA) or styrene (S) via a two-step ab initio emulsion process. *n*BA was first polymerized in water in the presence of the BlocBuilder alkoxyamine and DOWFAX 8390 as the surfactant to generate a stable aqueous suspension of living seeds of low molar mass P*n*BA-SG1. Seeded emulsion copolymerization was then performed via chain extension of the seeds at 110 °C for 8 h by a mixture of DOT and *n*BA (or S), leading to stable latexes of average diameters ranging from 120 to 320 nm. Successful degradations of the copolymers were achieved under basic conditions, which demonstrated the incorporation of labile thioester groups in the copolymer backbone.

Introduction

Emerging trends in the polymer field have turned to the development of more sustainable polymerization processes and materials to address pressing environmental issues.[1-2] In this context, conferring degradability and/or recyclability to polymer materials represents key strategies.[3-4] Vinyl polymers are a widespread class of polymers due to the broad diversity of monomers available, their ability to be functionalized and the variety of polymerization processes that can be used. However, they feature a carbon-carbon backbone, generally saturated and non-degradable, which favors their accumulation in the environment and prevents efficient recyclability and the establishment of a circular plastics economy. Radical polymerization methods exhibit numerous benefits for the synthesis of vinyl polymers, including benign reaction conditions, numerous polymerizable vinyl monomers and a wide range of homogeneous and heterogeneous polymerization processes.[5] The development of reversible-deactivation radical polymerization (RDRP) methods also enabled the synthesis of tailor-made, sophisticated macromolecular architectures with unprecedented properties and functionalities.[6-14]

The design of degradable vinyl polymers is the focus of great attention.[15] In the past few years, radical ring-opening polymerization (rROP) has witnessed a significant revival of interest as an efficient strategy to make traditional vinyl polymers degradable.[16-19] The rROP mechanism is based on the use of cyclic monomers that are capable of radical opening and are precursors of labile groups (e.g., ester) in the polymer backbone.[17] The main families of cyclic monomers used in rROP are cyclic ketene acetals (CKAs) and cyclic allylic sulfide lactones.[16-17] These monomers have been mainly employed as comonomers for the copolymerization with traditional vinyl monomers through the so-called "*cleavable comonomer*" approach. Although the resulting copolymers aim to challenge traditional polyesters, which are considered the gold standard,[20-21] the low reactivity of CKAs towards the vast majority of vinyl monomers, their high sensitivity towards protic solvents and water, as well as the occurrence of side reactions (e.g., cross linking) when using cyclic allylic sulfide lactones, make them uncompetitive.[16-17] For

instance, this prevents their polymerization in aqueous dispersed media to generate degradable latexes/particles in situ,[22] unless very specific conditions are used to prevent early hydrolysis of the CKA.[23] Developing such waterborne polymerization processes would also circumvent the limitations of traditional polyester nanoparticles that must be formulated from preformed polymers due to the impossibility of carrying out their synthesis under aqueous conditions.

Recently, thionolactones have emerged as a new family of rROP-compatible monomers. They are precursors of thioester groups in the main chain and exhibit key advantages compared to CKAs and cyclic allylic sulfide lactones.[24-33] In particular, dibenzo[c,e]oxepane-5-thione (DOT) has received growing interest[27-29, 32-37] due to its higher affinity towards acrylates[26, 28-29, 32, 34, 36] and other vinyl monomers,[27-30, 33, 38] its quantitative ring-opening, long storage and hydrolytic stability, as well as the possibility to be copolymerized under free-radical polymerization (FRP) and RDRP conditions.[28, 32, 34-37] Not only are thioester-containing copolymers interesting for post-functionalization or recycling purposes (e.g., via thiol-thioester exchange),[39] but they can also be degraded under various conditions including hydrolysis,[27, 36-37] aminolysis,[27-28, 32] methanolysis,[32] thiolysis,[33] or even under physiological conditions in the presence of cysteine or glutathione.[26, 37]

Due to its high hydrolytic stability, DOT has recently been successfully copolymerized with *n*-butyl acrylate (*n*BA) and/or styrene (S), by free-radical aqueous emulsion polymerization[29] and aqueous polymerization-induced self-assembly (PISA)[34, 36] from living water-soluble poly(acrylic acid),[34] poly(*N*-acryloylmorpholine)[36] or poly(ethylene glycol)[36] blocks. The resulting latexes were stable and the copolymers were degraded under different basic conditions. Herein, we have combined a waterborne RDRP process, that allows controlled copolymers to be obtained, with the avoidance of preliminary synthesis of living block in order to expand the range of heterogeneous polymerization processes capable of generating degradable latexes. We took advantage of a previously established strategy for producing living polymer chain particles by seeded emulsion polymerization[40] using a molecular

surfactant. Seeded emulsion polymerization is also known to be advantageous in terms of control of nucleation and particle number.[41] We thus report in this work the nitroxide-mediated seeded emulsion copolymerization of DOT and *n*BA or S to produce stable, well-defined copolymer latexes in situ (Figure 1), the copolymers of which can be successfully degraded under basic conditions.

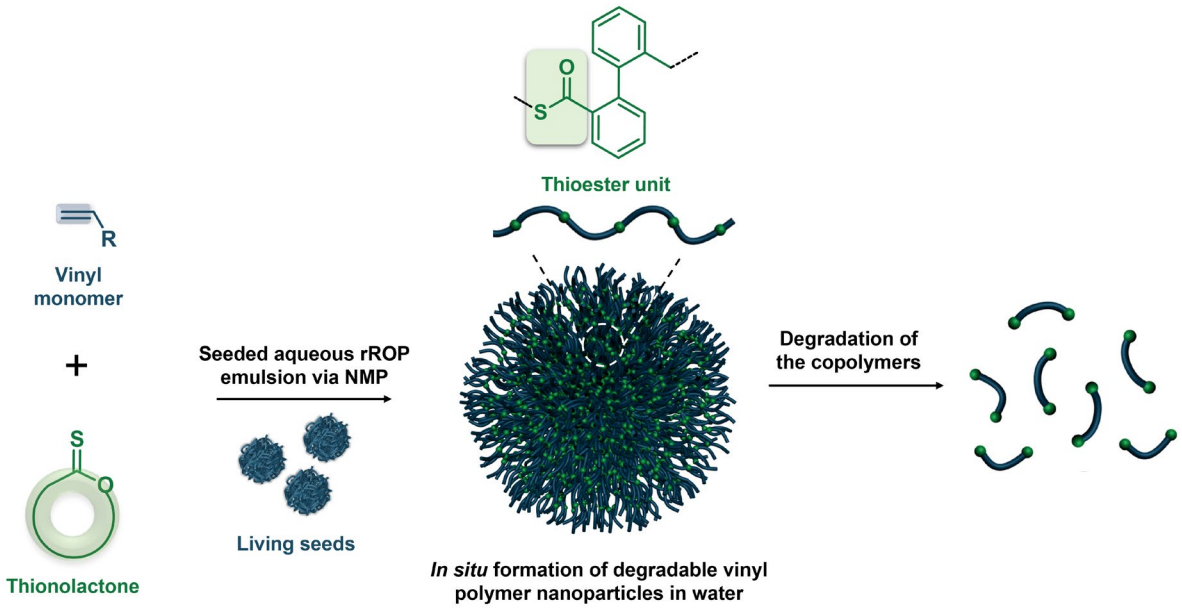

Figure 1. Synthesis of degradable latexes via nitroxide-mediated radical ring-opening copolymerization (rROP) of dibenzo[c,e]oxepane-5-thione (DOT) and vinyl monomers by nitroxide-mediated aqueous seeded emulsion polymerization.

Experimental section

Materials

n-Butyl acrylate (*n*BA, ≥ 99 %), styrene (S, ≥ 99 %), potassium hydroxide (KOH, 90 %), sodium hydrogen carbonate ($NaHCO_3$, ≥ 99 %) were purchased from Sigma-Aldrich and used as received. *N*-*tert*-butyl-*N*-(1-diethoxyphosphoryl-2,2-dimethylpropyl)aminoxy)-propionic acid alkoxyamine (BlocBuilder MA^{TM}, BB) was supplied by Arkema. 1,5,7-Triazabicyclo[4.4.0]dec-5-ene (TBD, >98 %) was purchased from TCI. Deuterated chloroform ($CDCl_3$) was purchased from Eurisotop. Chloroform ($CHCl_3$, HPLC grade) was obtained from VWR Chemicals.

Hydrochloric acid (HCl, 37 %) was supplied by Carlo-Erba. Dibenzo[c,e]oxepane-5-thione (DOT) was prepared as reported elsewhere using dibenzo[c,e]oxepin-5(7H)-one as intermediate.[28] Pressure glassware (round bottom flask 50 mL) was purchased from Sigma-Aldrich. DOWFAX 8390 was purchased from DOW.

Analytical Methods

Nuclear magnetic resonance (NMR) spectroscopy

NMR spectroscopy was performed in 5 mm diameter tubes in $CDCl_3$ at 25 °C. ^{1}H and ^{13}C NMR (udeft) spectroscopy was performed on a Bruker Avance 3 HD 400 spectrometer operating at 400 MHz. The chemical shift scale was calibrated based on the internal solvent signals (δ = 7.26 ppm) for $CDCl_3$.

Size exclusion chromatography (SEC)

SEC measurements were performed on a Tosoh EcoSEC HLC-8320 GPC with two columns from Agilent (PL-gel MIXED-D 300 ×7.5 mm, beads diameter 5 µm; linear part 400 to 400 000 g.mol^{-1}). Analyses were performed at 35 °C in chloroform (HPLC grade) at a flow-rate of 1 mL·min^{-1} using toluene as flow-rate marker. A conventional calibration curve was based on poly(methyl methacrylate) (PMMA) standards (peak molar masses: M_p = 625−625 500 g.mol^{-1}) or polystyrene (PS) standards (peak molar masses: M_p = 575–126 500 g.mol^{-1}) from Polymer Laboratories. This technique allowed M_n (number-average molar mass), M_w (weight-average molar mass), and M_w/M_n (dispersity, $Đ$) to be determined.

Dynamic light scattering (DLS)

Intensity-average nanoparticle diameter (D_z) and polydispersity index (PDI_{DLS}) were measured by DLS with a Nano ZS from Malvern (173° scattering angle) at a temperature of 25 °C. Copolymer dispersions were diluted in MilliQ water (dilution 1/10) prior to analysis.

Transmission electron microscopy (TEM)

The morphology of P*n*BA-*b*-P(S-*co*-DOT) nanoparticles was observed by TEM. Samples were diluted at 1 mg mL^{-1} in water just prior analysis (**D2** and **D0**, Table 1). 5 µL of diluted NPs dispersion were deposited on a 400-mesh carbon copper grid (Electron Microscopy Sciences). After 5 min at room temperature, a drop of phosphotungstic acid 2% filtered on 0.22 µm was added for negative staining during 30 s and the excess volume was removed with a blotting filter paper. The grids were then observed with a JEOL 1400 electron microscope operating at 80 kV. Digital images were directly recorded using a Gatan CCD camera using Digital Micrograph image acquisition and processing software (Gatan Inc.). The nanoparticles were analyzed by defining the number-average diameter ($D_{n,TEM}$), the weight-average diameter ($D_{w,TEM}$), the z-average diameter ($D_{z,TEM}$) and the polydispersity index (PDI_{TEM}) using equations described in Table S3.

Cryogenic transmission electron microscopy (cryo-TEM)

The morphology of P*n*BA-*b*-P(*n*BA-*co*-DOT) nanoparticles was observed by cryo-TEM. For analysis, 5 µL of NP suspension diluted at 20 mg mL^{-1} just prior analysis were deposited onto a 300 mesh carbon copper grid (Protochips). The excess was manually blotted with a filter paper, and the residual thin film was immediately frozen by plunging into liquid ethane cooled down at liquid nitrogen temperature using a Leica EM-CPC cryoplunger. Cryo-TEM images were acquired on a JEOL 1400 energy-filtered (20 eV) field emission gun electron microscope operating at 120 kV using a Gatan CCD camera. The nanoparticles were analyzed by defining

the number-average diameter ($D_{n,cryo\text{-}TEM}$), the weight-average diameter ($D_{w,cryo\text{-}TEM}$), the z-average diameter ($D_{z,cryo\text{-}TEM}$) and the polydispersity index ($PDI_{cryo\text{-}TEM}$), by using the same equations previously defined for TEM.

Synthetic procedures

*Synthesis of poly(n-butyl acrylate) seeds (PnBA) by nitroxide-mediated ab initio aqueous emulsion polymerization (**S0**)*

The experimental protocol was adapted from the work of Nicolas *et al.*[40] The polymerization was carried out in 50 mL-round-bottom pressure flask under nitrogen atmosphere stirred at 350 rpm with a magnetic bar. *n*BA (10 eq., 1.24 mmol, 0.16 g) was added into an aqueous phase comprising MilliQ water (20.45 mL), $NaHCO_3$ (26 mg, 12 $mmol.L_{aq}^{-1}$), the DOWFAX 8390 surfactant (0.578 g of surfactant solution, 15.4 $mmol.L_{aq}^{-1}$) and the BB alkoxyamine previously neutralized by NaOH (1 eq., 0.12 mmol, 0.047 g neutralized with an excess (1.65 eq.) of a 0.4 M sodium hydroxide solution). The solution was bubbled with dry argon to remove dissolved oxygen for 20 min at room temperature and then immersed in a preheated oil bath at 112 °C (giving 100 °C in the reaction medium) for 8 h. The solution was then rapidly cooled in an ice bath. The conversion of *n*BA was determined by gravimetry. SEC measurements were performed on dry extract. The latex was analysed by DLS.

*Synthesis of poly(n-butyl acrylate)-b-poly(n-butyl acrylate-co-dibenzo[c,e]oxepane-5-thione) (PnBA-b-P(nBA-co-DOT)) (**A0-C1**) by nitroxide-mediated aqueous seeded emulsion polymerization*

The experimental protocol was adapted from the work of Nicolas *et al.*[40] The polymerization was carried out in 50 mL-round-bottom pressure flask under nitrogen atmosphere stirred at 350 rpm with a magnetic bar. In a typical procedure (**A1**, Table 1), a mixture of *n*BA (2.4 mmol, 0.31 g) and DOT (0.024 mmol, 0.005 g, $f_{DOT,0}$ = 0.01) was added to the seed latex **S0** (6.67 g). The solution was bubbled with dry argon to remove dissolved oxygen for 20 min at room

temperature and then immersed in a preheated oil bath at 120 °C (giving 110 °C in the reaction medium) for 8 h. The solution was then rapidly cooled in an ice bath. The conversion of *n*BA was determined by gravimetry. The dry extracts were analysed by ^{1}H NMR in $CDCl_3$ and by SEC. The conversion of DOT was determined by ^{1}H NMR on the dry extract by integrating the 1H (Ar) of open DOT at 7.0 ppm and the 1H of DOT at 8.2 ppm. The latex was analysed by DLS and cryo-TEM.

The same procedure was adapted as follows by varying the initial monomer content (m_c^{th}) and the initial molar fraction of DOT ($f_{DOT,0}$): **A0** [**S0** (6.67 g), *n*BA (2.4 mmol, 0.31 g)]; **A2** [**S0** (6.67 g), *n*BA (2.4 mmol, 0.31 g) and DOT (0.05 mmol, 0.011 g, $f_{DOT,0}$ = 0.02)]; **B1** [**S0** (6.67 g), *n*BA (4.8 mmol, 0.62 g) and DOT (0.05 mmol, 0.011 g, $f_{DOT,0}$ = 0.01)] and **C1** [**S0** (6.67 g), *n*BA (7.3 mmol, 0.93 g) and DOT (0.07 mmol, 0.017 g, $f_{DOT,0}$ = 0.01)].

For kinetic monitoring, the same procedure was performed on the basis of **A1** with $f_{DOT,0}$ = 0.01. In five different 50 mL-round-bottom pressure flasks, the copolymerization of *n*BA and DOT was carried out for 1, 2, 4, 6 and 8 h.

*Synthesis of poly(n-butyl acrylate)-b-poly(styrene-co-dibenzo[c,e]oxepane-5-thione) (PnBA-b-P(S-co-DOT)) (**D0**, **D2**) by nitroxide-mediated aqueous seeded emulsion polymerization*

The experimental protocol was adapted from the work of Nicolas *et al.*[40] The polymerization was carried out in a 50 mL-round-bottom pressure flask under nitrogen atmosphere stirred at 350 rpm with a magnetic bar. In a typical procedure (**D2**, Table 1), a mixture of S (3 mmol, 0.31 g) and DOT (0.06 mmol, 0.014 g, $f_{DOT,0}$= 0.02) was added to the seed latex **S0** (6.67g). The solution was bubbled with dry argon to remove dissolved oxygen for 20 min at room temperature and then immersed in a preheated oil bath at 120 °C (giving 110 °C in the reaction medium) for 8 h. The solution was then rapidly cooled in an ice bath. The conversion of S was determined by gravimetry. Dry extract was analyzed by ^{1}H NMR in $CDCl_3$ and SEC. The latex was analyzed by DLS and TEM. A similar procedure was performed in absence of DOT (**D0**).

For kinetic monitoring, the same procedure was performed on the basis of **D2** with $f_{DOT,0}$ = 0.02. In six different 50 mL-round-bottom pressure flasks, the copolymerization of S and DOT was carried out for 1, 2, 3, 4, 6 and 8 h.

*Synthesis of poly(n-butyl acrylate)-b-poly(n-butyl acrylate-co-dibenzo[c,e]oxepane-5-thione)-b-poly(n-butyl acrylate-co-styrene-co-dibenzo[c,e]oxepane-5-thione) (PnBA-b-P(nBA-co-DOT)-b-P(nBA-co-S-co-DOT)) (**E1, E0**) by nitroxide-mediated aqueous seeded emulsion polymerization*

A seeded emulsion polymerization was performed as previously described for **A1** (Table 1), except that the polymerization was stopped after 4 h (*n*BA conversion = 20 wt.%) in order to maximize the livingness of the copolymer. The unreacted monomers were not removed. A fraction of S (0.021 g, 10 wt.% with respect to the overall required S) was added to the cooled latex, which was kept under stirring overnight to promote swelling of the particles. The remaining amount of S (0.195 g to reach 1:1 mol:mol of *n*BA and S in the final latex) was then added, followed by bubbling with argon for 20 min and heating at 120 °C (giving 110 °C in the reaction medium) for 9 h. The overall conversion of *n*BA and S was determined by gravimetry. The dry extract was analyzed by ^{1}H NMR in $CDCl_3$ and SEC. The latex was analyzed by DLS. A similar procedure was performed in absence of DOT (**E0**).

Degradation procedures

Degradation of the copolymers by TBD

10 mg of dry extract was solubilized in 0.5 mL of THF for 2 h before adding 0.5 mL of solution at 5 wt.% TBD in THF. The solution was stirred for 16 h at room temperature. The degradation reaction was quenched with a HCl solution (1 M) to reach a neutral pH and the sample was dried under vacuum until constant weight. The degradation products were analyzed by SEC.

Results and Discussion

Degradable vinyl polymer nanoparticles were synthesized by aqueous seeded emulsion copolymerization of DOT and *n*BA or S via NMP in presence of DOWFAX 8390 as a surfactant (Figure 2).

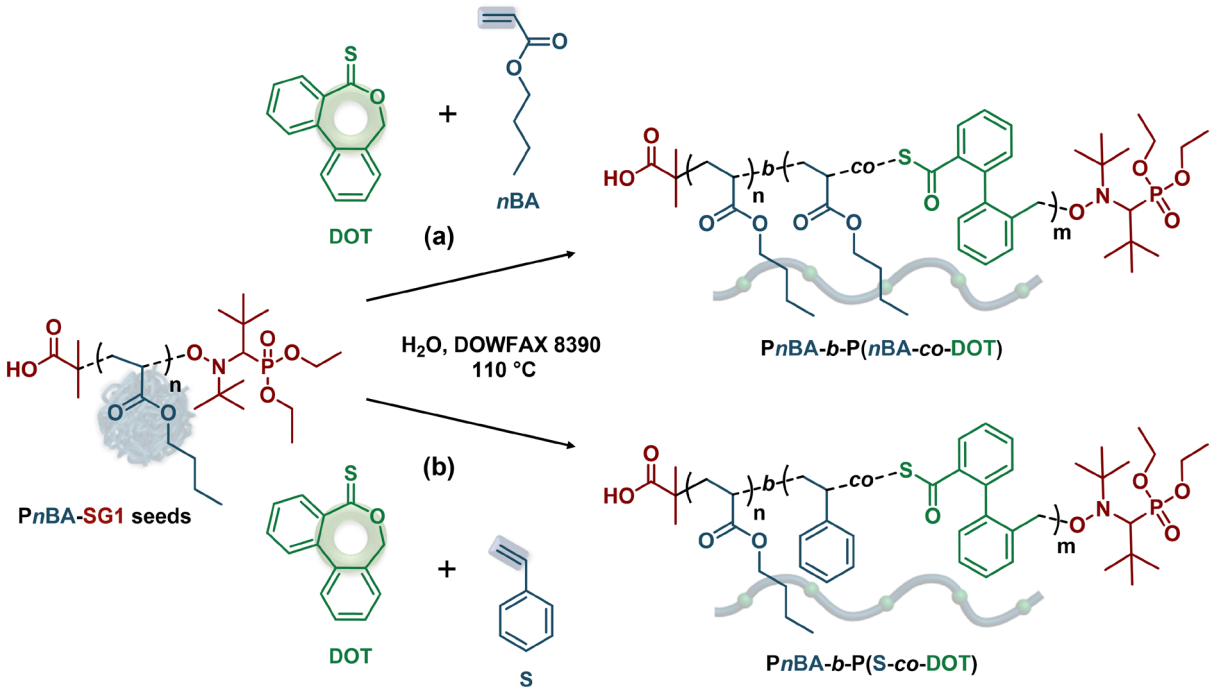

Figure 2. Synthesis of: (a) poly(*n*-butyl acrylate)-*b*-poly(*n*-butyl acrylate-*co*-dibenzo[c,e]oxepane-5-thione) (P*n*BA-*b*-P(*n*BA-*co*-DOT)) and (b) poly(*n*-butyl acrylate)-*b*-poly(styrene-*co*-dibenzo[c,e]oxepane-5-thione) (P*n*BA-*b*-P(S-*co*-DOT)) diblock copolymer latexes by nitroxide-mediated radical ring-opening copolymerization (rROP) of DOT and *n*BA (or S) via aqueous seeded emulsion polymerization from a living P*n*BA-SG1 seed.

An aqueous *ab initio* nitroxide-mediated emulsion polymerization of *n*BA was first performed for 8 h at 100 °C to form the living seeds. A low concentration of monomer was considered (theoretical solids content, τ^{th} = 0.7 wt.%) together with a large concentration of surfactant (~20 times its critical micellar concentration), similar to a microemulsion polymerization, to prevent unwanted droplet nucleation. As previously demonstrated,[40] direct *ab initio* emulsion polymerization with the whole amount of *n*BA led to unstable latex after 50 % of conversion.

Thus, using living seeds can prevent coagulum formation and favour the formation of stable latexes at higher solids content after addition of a second batch of monomer. The P*n*BA-SG1 seeds were obtained with a conversion of ~50 % to maintain a high livingness and exhibited great colloidal stability with D_z = 153 nm and a PDI_{DLS} = 0.19 (Table 1). We also targeted a low M_n value (M_n = 900 g.mol^{-1}) so as not to adversely affect the macromolecular characteristics of the copolymer after degradation. They were then chain-extended to reach higher solids content latexes by addition of a mixture of DOT and *n*BA (or S). Various τ^{th} values, from 4.5 to 12.3 wt.%, were investigated to evaluate the robustness of the polymerization process (Table 1). According to the solubility of DOT in the comonomer, initial molar fractions of 1 and 2 mol.% were studied.

Table 1. Experimental conditions and macromolecular characteristics for the synthesis of P*n*BA-*b*-P(*n*BA-*co*-DOT) and P*n*BA-b-P(S-*co*-DOT) diblock copolymer latexes obtained by aqueous seeded emulsion rROP.

Entry	Monomer	$f_{DOT,0}$ [a] (mol.%)	τ^{th} (wt.%)	T (°C)	$DP_{n,th}$ [b]	Conv. *n*BA/S[c] (wt.%)	$M_{n,th}$ [d] (g.mol^{-1})	M_n [e] (g.mol^{-1})	$Đ$ [e]	D_z [f] (nm)	PDI_{DLS} [f]	F_{DOT} [g] (mol.%)	f [h]
S0	**seed latex (*n*BA)**	0	0.7	100	10	50	1 000	900	1.14	153	0.19	0	-
A0		0	4.5	110	64	72	7 000	8 800	1.62	210	0.54	0	0.77
A1		1.0	4.5	110	64	63	6 200	8 600	1.63	153	0.47	0.8	0.69
A2	***n*BA**	2.0	4.5	110	64	71	6 700	7 900	1.62	320	0.48	2.0	0.83
B1		1.0	8.5	110	129	80	14 300	26 000	1.57	187	0.43	0.8	0.53
C1		1.0	12.3	110	192	80	20 600	47 900	1.72	290	0.50	0.9	0.42
D0	**S**	0	4.5	110	77	82	7 200	10 300	1.18	139	0.48	n.d.	0.61
D2		2.0	4.5	110	77	76	6 800	10 300	1.38	122	0.47	n.d.	0.57
E0[i]	(1) ***n*BA**	0	7.0	110	124	43	16 500	13 700	1.20	174	0.36	0	1.25
E1[i]	(2) **S**	1.0	7.0	110	124	47	16 800	15 800	1.20	166	0.39	n.d.	1.08

[a] Initial molar fraction of DOT in the reaction medium. [b] Theoretical DP_n for *n*BA or S. [c] Determined by gravimetry. [d] Determined according to: $M_{n,th} = M_{n,PnBA\text{-}SG1} + DP_{n,th}$ x conv. x $MW_{nBA\ or\ S}$. [e] Determined by SEC in $CHCl_3$ on dry extract. [f] Determined by DLS. [g] Determined by ^{1}H NMR on the dry extract by integrating the 1H (Ar) of open DOT at 7.0 ppm and the 3H of (-CH3) of P*n*BA at 0.9 ppm. Aromatic peaks of DOWFAX 8390 surfactant were considered as negligeable for the integration of the DOT aromatic protons (Figure S2). For P*n*BA-*b*-P(S-*co*-DOT), determination of F_{DOT} was not possible as previously reported,[34] because of the 2H in α-position to the ester of *n*BA units at 4 ppm. [h] Initiation efficiency, determined according to: $f = (M_{n,th} - M_{n,PnBA\text{-}SG1}) / (M_n - M_{n,PnBA\text{-}SG1})$. [i] A first polymerization of *n*BA (+DOT for **E1**) was performed from P*n*BA-SG1 seeds and then chain-extended with S.

Copolymerization of DOT ($f_{DOT,0}$ = 0.01) with *n*BA at a solids content of 4.5 wt.% ($DP_{n,th}$ = 64) was first considered (**A1**, Figure 3a, Table 1). After 8 h of polymerization, 63 % conversion in *n*BA was obtained, giving M_n = 8.6 kg.mol^{-1}, $Đ$ = 1.63, and an initiation efficiency (f) of 0.69, which is comparable to the same experiment performed in absence of DOT (**A0**, Table 1). Importantly, after the reaction, the initially yellow emulsion turned into a stable milky white latex (Figure S1). Such a change in colour is characteristic of the isomerization of DOT upon polymerization, leading to a colourless thioester, as previously mentioned by Smith and co-

workers.[32] A complete conversion in DOT was reached after 4 h (Figure 3a) and its successful insertion into the P*n*BA backbone was confirmed by ^{1}H NMR spectroscopy of dry extracts showing a displacement of the aromatic peaks from DOT to a lower chemical shift of 7.0–8.0 ppm, characteristic of open DOT units (Figure 3b).[34] By integrating the aromatic protons of DOT at 7.0 ppm (peak *g*) and the methyl protons of P*n*BA at 0.9 ppm (peak *a*), the molar fraction of DOT in the copolymer (F_{DOT}) reached 0.8 mol.% (Figure 3b). Note that the aromatic peaks of DOWFAX 8390 were considered as negligeable for the integration of the aromatic protons of DOT (Figures 3b and S2). The controlled nature of the copolymerization for **A1** was confirmed by the linear evolution of M_n with *n*BA conversion with rather narrow dispersity, despite its progressive increase throughout the polymerization (Figure 3c). The M_n values were also close to the predicted ones. Interestingly, F_{DOT} decreased from 4.5 to 0.8 mol.% during the copolymerization, which is explained by the faster consumption of DOT when copolymerized with acrylates (Figure 3a),[28-29] thus leading to gradient-type copolymers. These data are in line with previous results obtained by aqueous nitroxide-mediated rROPISA of DOT and *n*BA.[34]

The initial DOT content in the comonomer feed was then doubled ($f_{DOT,0}$ = 0.02) (**A2**, Table 1). No significant variation was obtained in terms of reaction kinetics or control of the copolymerization compared to **A1** as M_n = 7.9 kg.mol^{-1} and $Đ$ = 1.62 (Table 1). As expected, a greater insertion of DOT units was achieved up to 2 mol.% (Table 1 and Figure 3b).

The $DP_{n,th}$ value was then progressively increased from 64 to 192 to evaluate the working range of the seeded aqueous emulsion polymerization process (**A1**–**C1**, Table 1). As expected, this resulted in a progressive increase of the M_n from 8 600 to 47 900 g.mol^{-1} (Table 1). A slight increase of the dispersities was noticed, which may be assigned to higher *n*BA conversions (~80%) that promoted irreversible termination and intermolecular chain transfer to polymer, often seen with this monomer.[40, 42-43] Note that the same trend was observed in absence of DOT (**A0**–**C0**, Table S1), thus ruling out a potential detrimental effect of the thionolactone on the control of the polymerization. It could be noticed that experiment **C1** with 12.5 wt.%

monomer content gave rise to formation of a small fraction of coagulum on the side of the flask at the emulsion/air interface, which illustrates the limitations of our experimental setup.

Figure 3. Synthesis of P*n*BA-*b*-P(*n*BA-*co*-DOT) copolymer latexes by copolymerization of *n*BA and DOT in water at 110 °C initiated by P*n*BA-SG1 seeds (**A1**, Table 1): (a) evolution of *n*BA conversion, DOT conversion and average molar fraction of DOT (F_{DOT}) in the copolymer vs. time; (b) ^{1}H NMR spectra (400 MHz, $CDCl_3$) in the 0–8 ppm region of P*n*BA-*b*-P(*n*BA-*co*-DOT) copolymers **A0**, **A1** and **A2**; (c) evolution of M_n and $Đ$ vs. *n*BA conversion (**A1**).

From the colloidal viewpoint, stable but polydisperse latexes **A1**–**C1** were observed by DLS (PSD_{DLS} > 0.4) in agreement with previous work using such two-step emulsion polymerization process (Table 1 and Figure 4a).[40] Note that DLS measurements were performed without any filtration to give representative values of the average diameters and PDI_{DLS}. D_z values ranging from 153 to 320 nm were reported. However, due to the high polydispersities of the latexes and the inability of the DLS apparatus to precisely capture the particle size distribution of broadly dispersed nanoparticle suspensions, D_z values are considered not accurate. Nonetheless, the average diameters were constant with only little variation after one month for **A0** and **A1** (Figures 4a and S3), demonstrating the high colloidal stability of the latexes. Cryo-TEM analysis revealed spherical morphologies (Figure 4b) and confirmed the broad particle size distribution as $D_{n,cryo\text{-}TEM}$ = 71 nm, $D_{w,cryo\text{-}TEM}$ = 357 nm and $PDI_{cryo\text{-}TEM}$ = 5 for **A1**. Note that very similar colloidal properties were determined for **A0**, which confirmed once again the minimal influence of DOT despite its strong hydrophobicity (Table S2).

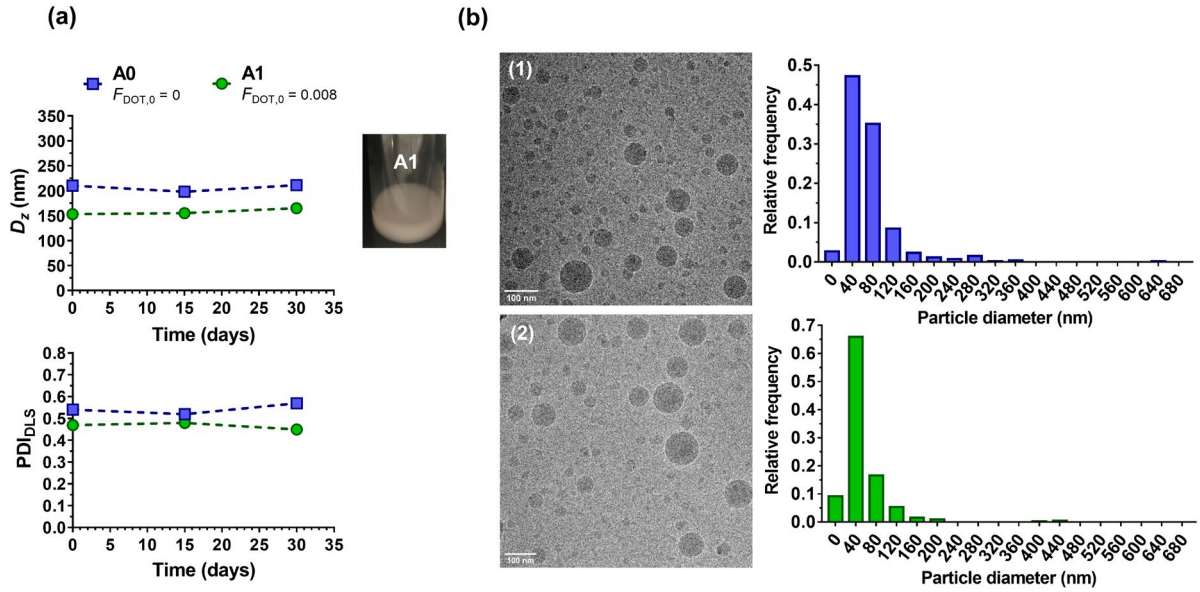

Figure 4. Colloidal properties of P*n*BA-*b*-P(*n*BA-*co*-DOT) copolymer latexes (**A0** and **A1**, Table 1). (a) Variation of the intensity-average diameter (D_z) and the polydispersity index (PDI_{DLS}) with time measured by DLS. (b) Representative cryo-TEM images and associated particle size distribution (n = 500) for latexes: (1) **A0** and (2) **A1**.

We then adapted the aqueous seeded emulsion polymerization process to the synthesis of P*n*BA-*b*-P(S-*co*-DOT) copolymer latexes. An initial molar fraction of DOT of 2 mol.% was used due to its slightly higher solubility in S, with a τ^{th} of 4.5 wt.% (**D2**, Table 1). After 8 h of polymerization from the living P*n*BA-SG1 seeds **S0**, 76 % conversion in S was reached, which was comparable to the same experiment performed in absence of DOT (**D0**, Table 1 and Figure 5a). Both experiments resulted in copolymers of M_n = 10.3 kg.mol^{-1} with relatively low dispersity ($Đ$ = 1.18 and 1.38, respectively), even though the presence of DOT may have affected the molar mass distribution (Table 1). By ^{1}H NMR, no characteristic peak of unreacted DOT was observed at 8.2 ppm after 8 h of copolymerization, proving its full incorporation in the copolymer (Figure 5b). Visually speaking, the latex turned from yellow to white, similarly to what has been observed for **A1**. However, insertion of thioester units was not possible to be quantified by ^{1}H NMR because of the methylenic protons from P*n*BA at 4 ppm (peak *g*, Figure 5b). Other analytical methods, such as carbon NMR spectroscopy or SEC (with a UV detector) of **D2** also did not clearly reveal the presence of thioester units in the PS backbone due to the

low $f_{DOT,0}$ considered: no characteristic peak of O=C-S function at 190 ppm was detected by ^{13}C NMR (Figure S4), nor UV signal on the SEC chromatogram of P*n*BA-*b*-P(S-*co*-DOT) copolymer at a specific wavelength of open DOT (λ = 330 nm).[31] Nonetheless, by analogy with our previous work on PAA-*b*-P(S-*co*-DOT) latexes obtained by rROPISA,[34] the incorporation of DOT was estimated at about 3 mol.%. The rather linear evolution of M_n with S conversion and the low dispersity values for **D2** were shown (Figure 5c), attesting to the controlled nature of the copolymerization.

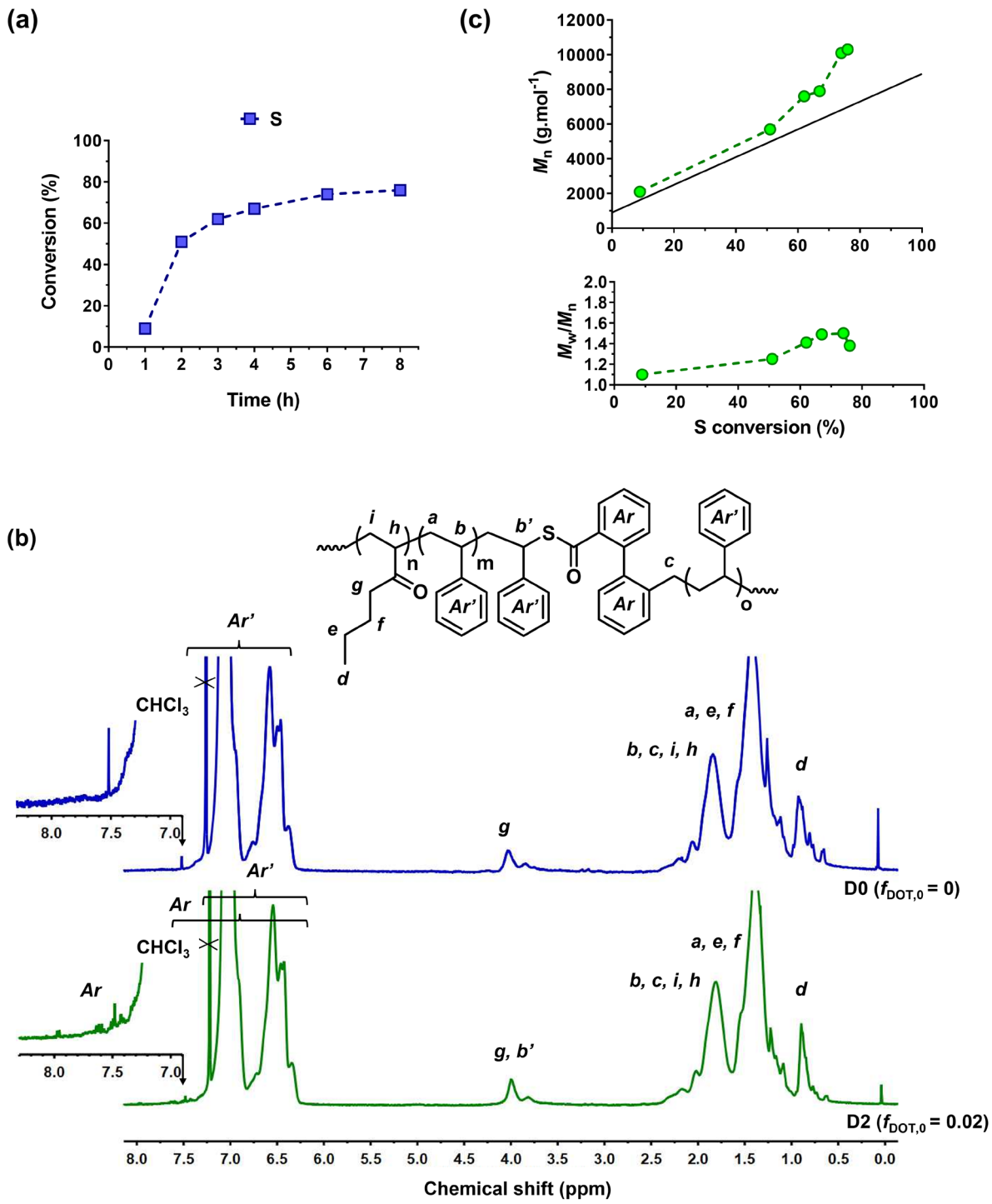

Figure 5. Synthesis of P*n*BA-*b*-P(S-*co*-DOT) copolymer latexes by copolymerization of S and DOT in water at 110 °C initiated by P*n*BA-SG1 seeds (**D2**, Table 1): (a) evolution of S conversion, DOT conversion and average molar fraction of DOT (F_{DOT}) in the copolymer vs. time; (b) ^{1}H NMR spectra (400 MHz, $CDCl_3$) in the 0–8 ppm region of P*n*BA-*b*-P(S-*co*-DOT) copolymers **D0** and **D2** and (c) evolution of M_n and $Đ$ vs. S conversion.

Like for *n*BA, stable but polydisperse P*n*BA-*b*-P(S-*co*-DOT) copolymer latexes with D_z values ranging from 122 to 139 nm were obtained according to DLS measurements (**D0** and **D2**, Table 1, Figure 6a). TEM analysis of **D0** and **D2** revealed $D_{n,TEM}$ values of about 40 nm, as attested from the significant fraction of small particles on TEM images (Table 1 and S3, Figure 6b). They also featured a spherical morphology with a confirmed broad particle distribution. For instance, **D2** exhibited $D_{w,TEM}$ = 166 nm and PDI_{TEM} = 3.9 (Table S3). Nevertheless, these latexes also demonstrated a remarkable colloidal stability over at least one month (Figure 6a and 4a).

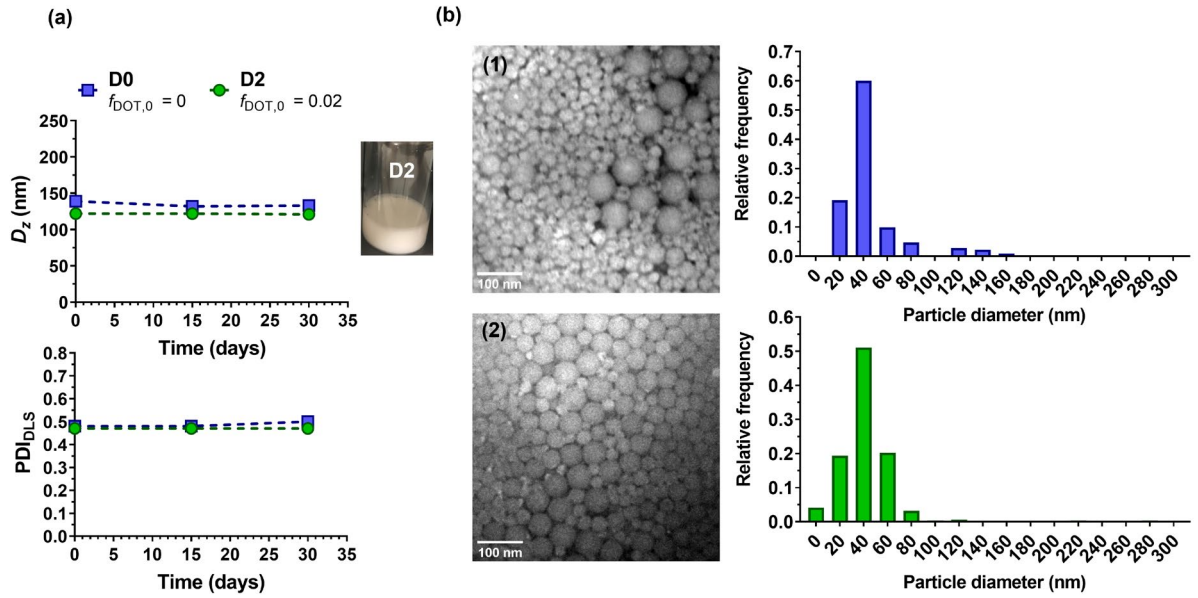

Figure 6. Colloidal properties of P*n*BA-*b*-P(S-*co*-DOT) copolymer latexes (**D0** and **D2**, Table 1). (a) Variation of the intensity-average diameter (D_z) and the polydispersity index (PDI_{DLS}) with time measured by DLS. (b) Representative TEM images and associated size distribution (n = 500) for latexes: (1) **D0** and (2) **D2**.

To confirm the degradability of the copolymers, the dry extracts were treated under basic conditions. TBD was selected as the base soluble in both water and THF, as previously described for the degradation of PAA-*b*-P(*n*BA-*co*-DOT) latexes.[34] For *n*BA-based copolymers **A1**–**C1**, successful degradation was demonstrated after 16 h in presence of 2.5 wt.% TBD (Table 2). While **A1** copolymer exhibited a M_n loss of 13 % (Table 2 and Figure 7a), rising F_{DOT} up to 0.02 (**A2**) led to a higher M_n loss of nearly 30 % (**A2**, Table 2, Figure 7b). Conversely, the

M_n of P*n*BA homopolymer **A0** after degradation under identical conditions stayed constant (Figure S5a, Table 2), which confirmed the successful insertion of thioester units into P*n*BA backbone when DOT is copolymerized with *n*BA. Importantly, increasing $DP_{n,PnBA}$ led to a higher M_n and to a higher M_n loss: -50 % for **B1** and -68 % for **C1** (Table 2, Figure 7c and d). The result might be explained by both the propensity to obtain a gradient copolymer during the copolymerization of DOT and *n*BA, and by the more spread-out insertion of DOT when the targeted M_n is higher. Influence of the solids content might also play a role in terms of diffusion of the monomer/repartition of DOT units. Importantly, all M_n values after degradation were in good agreement with the theoretical M_n of the degraded copolymers ($M_{n,deg.th}$, Table 1).

Regarding P*n*BA-*b*-P(S-*co*-DOT) copolymer **D2**, a decrease in M_n of 28 % was reached on after 16 h, which is comparable to the degradation of copolymer **A2** (Table 2 and Figure 7e). This relatively moderate loss in M_n could be explained by the stronger gradient character in the P(S-*co*-DOT) block compared to its *n*BA counterpart. As expected, degradation of P*n*BA-*b*-PS copolymer under the same experimental conditions did not lead to measurable decrease in M_n (Figure S5b).

Table 1. Macromolecular characteristics of P*n*BA-*b*-P(*n*BA-*co*-DOT) and P*n*BA-*b*-P(S-*co*-DOT) copolymer latexes obtained by aqueous seeded emulsion rROP and their degradation products obtained under basic conditions.

Entry	Monomer	$f_{DOT,0}$ (mol.%)	F_{DOT} (mol.%)	M_n [a] (g.mol^{-1})	$Đ$ [a]	$M_{n,deg.th}$ [b] (g.mol^{-1})	$M_{n,\ deg\ TBD}$ [c] (g.mol^{-1}) (% M_n loss)
A0	***n*BA**	0	0	8 800	1.62	8 800	8 700 (- 1 %)
A1		1.0	0.8	8 600	1.63	5 400	7 500 (- 13 %)
A2		2.0	2.0	7 900	1.62	3 500	5 600 (- 29 %)
B1		1.0	0.8	26 000	1.57	9 900	13 100 (- 50 %)
C1		1.0	0.9	47 900	1.72	11 100	15 500 (- 68 %)
D0	**S**	0	n.d.	10 300	1.18	n.d.	10 400 (- 0 %)
D2		2.0	n.d.	10 300	1.38	n.d.	7 400 (- 28 %)
E1[d]	(1) ***n*BA** (2) **S**	1.0	n.d.	15 800	1.20	n.d.	13 500 (- 14 %)

[a] Determined by SEC in $CHCl_3$ on dry extract. [b] Determined according to: $M_{n,deg.th} = [(1 / ((1 / DP_n) + (F_{DOT} / (1 - F_{DOT})))) \times MW_{nBA}] + MW_{DOT}$ with $DP_n = (M_n - M_{n,PnBa\text{-}SG1}) / ((F_{DOT} \times MW_{DOT}) + (F_{nBA} \times MW_{nBA}))$. [c] Determined by SEC in $CHCl_3$ after degradation on dry extract dissolved at 10 mg.mL^{-1} in solution at 2.5 wt.% of TBD in THF for 16 h. [d] A first (co)polymerization of *n*BA (+DOT for **E1**) was performed from P*n*BA-SG1 seeds and then chain-extended with S.

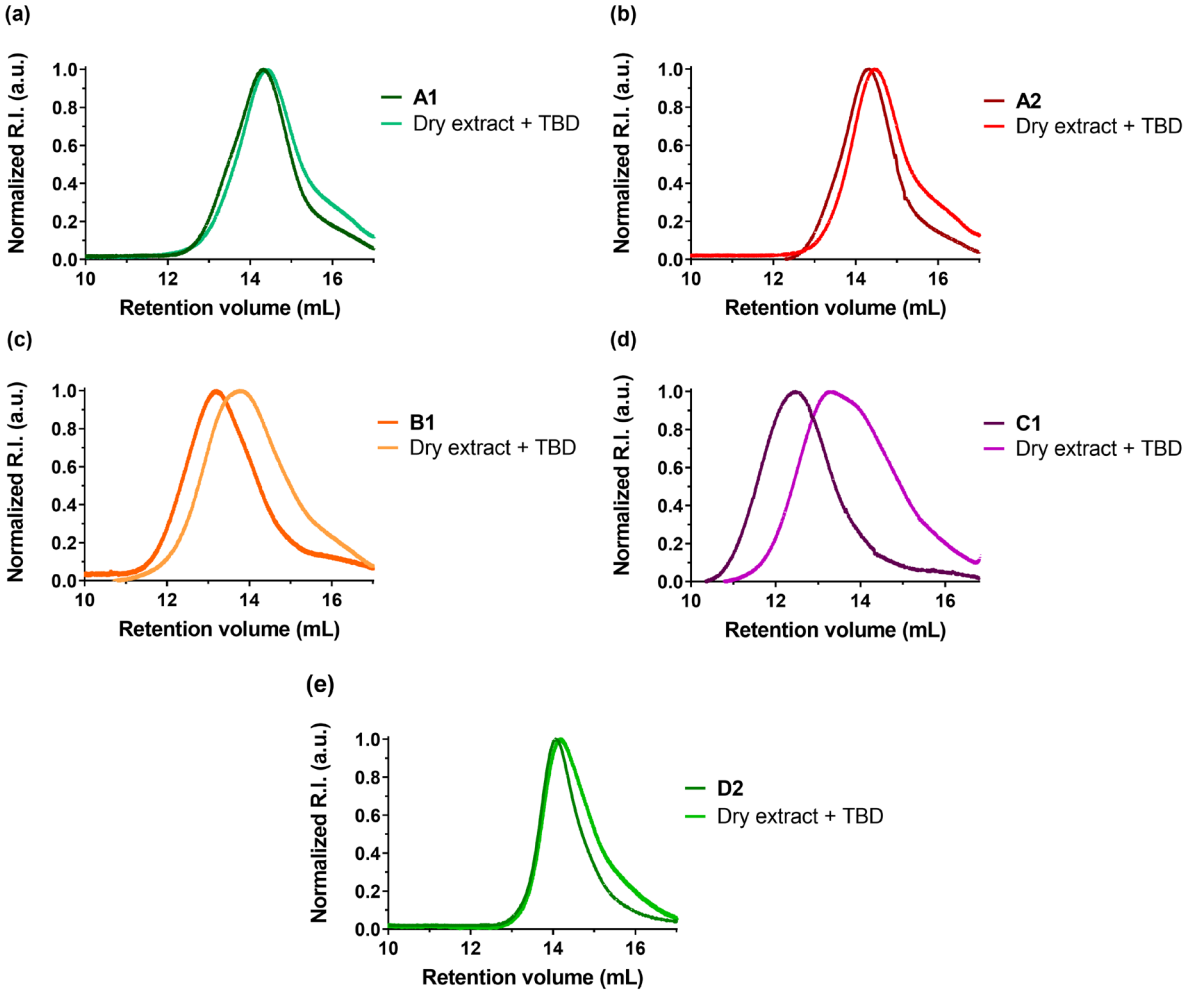

Figure 4. Evolution of SEC chromatograms of P*n*BA-*b*-P(*n*BA-*co*-DOT) copolymers: (a) **A1**, (b) **A2**, (c) **B1**, (d) **C1** (Table 1) and P*n*BA-*b*-P(S-*co*-DOT) copolymer (e) **D2** (Table 1), after degradation of dry extracts by TBD.

The process was then applied to the synthesis of a P*n*BA-*b*-P(*n*BA-*co*-DOT)-*b*-PS triblock copolymer latex by a three-step synthesis consisting in the chain extension of the P*n*BA-*b*-P(*n*BA-*co*-DOT) copolymer latex with S (equimolar ratio was considered between *n*BA and S). The seeded emulsion copolymerization of DOT and *n*BA was performed from the seed latex **S0** at 110 °C but for only 4 h (20% in *n*BA conversion) in order to maintain a high livingness of the P(*n*BA-*co*-DOT) chains. The newly formed latex **E1'** was then cooled down at room temperature and 10 wt.% of the final S amount was added for an overnight swelling. After the addition of the remaining fraction of S, the polymerization was resumed for an additional 9 h,

producing the latex **E1**. A final conversion of 47 % was obtained by gravimetry by taking into account the residual amounts of *n*BA. Successful reinitiation of the P*n*BA-*b*-P(*n*BA-*co*-DOT) latex **E1'** was achieved, as demonstrated by SEC analysis which indicated a complete shift of the SEC trace towards higher M_n values (Figure 8a). Polydisperse nanoparticles suspension with a size about 160 nm was observed by DLS (Table 1). Degradation with TBD of intermediate copolymer **E1'** and final copolymer **E1** evidenced the incorporation of thioester units in the copolymer structure (Figures 8b, S6 and S7). Despite the modest degradation because of the synthesis of a gradient copolymer (thus inducing cleavage on the side of the short macroinitiator), this experiment demonstrated the possibility of achieving triblock copolymer latexes by NMP that comprised a degradable block.

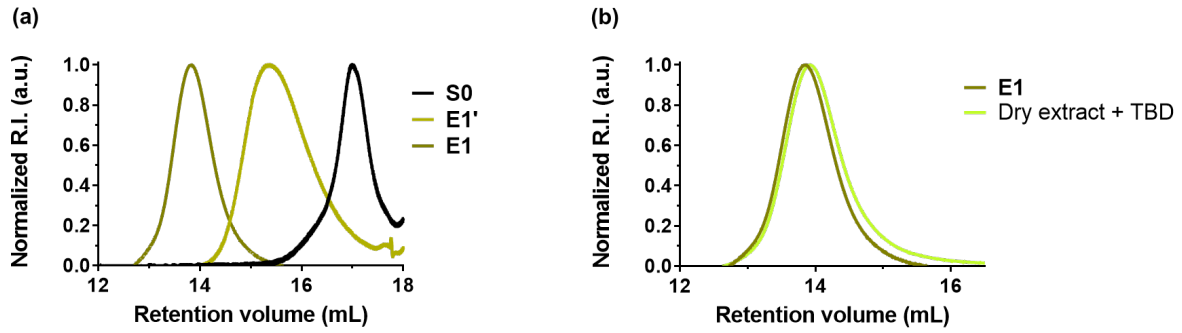

Figure 5. SEC chromatograms of (a) P*n*BA (**S0**), P*n*BA-*b*-P(*n*BA-*co*-DOT) (**E1'**) copolymers and chain extension of **E1'** with styrene (**E1**), and (b) evolution of SEC chromatogram of **E1** copolymer after treatment with TBD (Table 2).

Conclusion

Aqueous seeded emulsion copolymerization of DOT and *n*BA (or S) was successfully achieved via NMP. Remarkable colloidal stability of the latexes was demonstrated up to one month. Variations of the targeted $DP_{n,PnBA}$ or $f_{DOT,0}$ resulted in M_n values from 8 600 to 47 900 g.mol^{-1}. ^{1}H NMR spectroscopy demonstrated the successful insertion of thioester units into P*n*BA backbone from 0.8 to 2 mol.%, and the more favorable insertion of DOT compared to *n*BA (or S), in agreement with the reported reactivity ratios. Significant degradation of both copolymers

P*n*BA-*b*-P(*n*BA-*co*-DOT) and P*n*BA-*b*-P(S-*co*-DOT) were demonstrated with TBD. Successful chain extension of P*n*BA-*b*-P(*n*BA-*co*-DOT) latex with S was also demonstrated. This fully aqueous polymerization process allowed for the formation of stable and degradable vinyl copolymer latexes in situ without additional synthesis of purification step.

Acknowledgments

The authors acknowledge the financial support from the Agence Nationale de la Recherche (grant number ANR-18-CE06-0014 CKAPART). This work has benefited from the platform and expertise of the Electron Microscopy Facility of I2BC, Gif-sur-Yvette.

References

1. Fagnani, D. E.; Tami, J. L.; Copley, G.; Clemons, M. N.; Getzler, Y. D. Y. L.; McNeil, A. J., 100th Anniversary of Macromolecular Science Viewpoint: Redefining Sustainable Polymers. *ACS Macro Lett.* **2021,** *10* (1), 41-53.
2. Ashe, K., The steps to sustainability. *Nat. Chem.* **2022,** *14* (3), 243-244.
3. Rahimi, A.; García, J. M., Chemical recycling of waste plastics for new materials production. *Nature Reviews Chemistry* **2017,** *1* (6), 0046.
4. Korley, L. T. J.; Epps, T. H.; Helms, B. A.; Ryan, A. J., Toward polymer upcycling—adding value and tackling circularity. *Science* **2021,** *373* (6550), 66-69.
5. Matyjaszewski, K.; Davis, T. P., *Handbook of radical polymerization*. John Wiley & Sons: 2003.
6. Nicolas, J.; Guillaneuf, Y.; Lefay, C.; Bertin, D.; Gigmes, D.; Charleux, B., Nitroxide-mediated polymerization. *Prog. Polym. Sci.* **2013,** *38* (1), 63-235.
7. Shanmugam, S.; Matyjaszewski, K., Reversible Deactivation Radical Polymerization: State-of-the-Art in 2017. In *Reversible Deactivation Radical Polymerization: Mechanisms and Synthetic Methodologies*, American Chemical Society: 2018; Vol. 1284, pp 1-39.
8. Scholten, P. B. V.; Moatsou, D.; Detrembleur, C.; Meier, M. A. R., Progress Toward Sustainable Reversible Deactivation Radical Polymerization. *Macromol. Rapid Commun.* **2020,** *41* (16), 2000266.
9. Corrigan, N.; Jung, K.; Moad, G.; Hawker, C. J.; Matyjaszewski, K.; Boyer, C., Reversible-deactivation radical polymerization (Controlled/living radical polymerization): From discovery to materials design and applications. *Prog. Polym. Sci.* **2020,** *111*, 101311.
10. Perrier, S., 50th Anniversary Perspective: RAFT Polymerization—A User Guide. *Macromolecules* **2017,** *50* (19), 7433-7447.
11. Nothling, M. D.; Fu, Q.; Reyhani, A.; Allison-Logan, S.; Jung, K.; Zhu, J.; Kamigaito, M.; Boyer, C.; Qiao, G. G., Progress and Perspectives Beyond Traditional RAFT Polymerization. *Advanced Science* **2020,** *7* (20), 2001656.

12. Grubbs, R. B., Nitroxide-Mediated Radical Polymerization: Limitations and Versatility. *Polymer Reviews* **2011,** *51* (2), 104-137.

13. Matyjaszewski, K.; Tsarevsky, N. V., Macromolecular Engineering by Atom Transfer Radical Polymerization. *J. Am. Chem. Soc.* **2014,** *136* (18), 6513-6533.

14. Matyjaszewski, K., Advanced Materials by Atom Transfer Radical Polymerization. *Adv. Mater.* **2018,** *30* (23), 1706441.

15. Delplace, V.; Nicolas, J., Degradable vinyl polymers for biomedical applications. *Nature Chem.* **2015,** *7* (10), 771-784.

16. Pesenti, T.; Nicolas, J., 100th Anniversary of Macromolecular Science Viewpoint: Degradable Polymers from Radical Ring-Opening Polymerization: Latest Advances, New Directions, and Ongoing Challenges. *ACS Macro Lett.* **2020,** *9* (12), 1812-1835.

17. Tardy, A.; Nicolas, J.; Gigmes, D.; Lefay, C.; Guillaneuf, Y., Radical Ring-Opening Polymerization: Scope, Limitations, and Application to (Bio)Degradable Materials. *Chem. Rev.* **2017,** *117* (3), 1319-1406.

18. Jackson, A. W., Reversible-deactivation radical polymerization of cyclic ketene acetals. *Polym. Chem.* **2020,** *11* (21), 3525-3545.

19. Agarwal, S., Chemistry, chances and limitations of the radical ring-opening polymerization of cyclic ketene acetals for the synthesis of degradable polyesters. *Polym. Chem.* **2010,** *1* (7), 953-964.

20. Washington, K. E.; Kularatne, R. N.; Karmegam, V.; Biewer, M. C.; Stefan, M. C., Recent advances in aliphatic polyesters for drug delivery applications. *WIREs Nanomedicine and Nanobiotechnology* **2017,** *9* (4), e1446.

21. Liechty, W. B.; Kryscio, D. R.; Slaughter, B. V.; Peppas, N. A., Polymers for Drug Delivery Systems. *Annu. Rev. Chem. Biomol. Eng.* **2010,** *1* (1), 149-173.

22. Zhu, C.; Denis, S.; Nicolas, J., A Simple Route to Aqueous Suspensions of Degradable Copolymer Nanoparticles Based on Radical Ring-Opening Polymerization-Induced Self-Assembly (rROPISA). *Chem. Mater.* **2022,** *34* (4), 1875-1888.

23. Galanopoulo, P.; Sinniger, L.; Gil, N.; Gigmes, D.; Lefay, C.; Guillaneuf, Y.; Lages, M.; Nicolas, J.; D'Agosto, F.; Lansalot, M., Degradable vinyl polymer particles by radical aqueous emulsion copolymerization of methyl methacrylate and 5,6-benzo-2-methylene-1,3-dioxepane. *Polym. Chem.* **2023,** *14* (11), 1224-1231.

24. Ivanchenko, O.; Authesserre, U.; Coste, G.; Mazières, S.; Destarac, M.; Harrisson, S., ε-Thionocaprolactone: an accessible monomer for preparation of degradable poly(vinyl esters) by radical ring-opening polymerization. *Polym. Chem.* **2021,** *12* (13), 1931-1938.

25. Plummer, C. M.; Gil, N.; Dufils, P.-E.; Wilson, D. J.; Lefay, C.; Gigmes, D.; Guillaneuf, Y., Mechanistic Investigation of ε-Thiono-Caprolactone Radical Polymerization: An Interesting Tool to Insert Weak Bonds into Poly(vinyl esters). *ACS Applied Polymer Materials* **2021,** *3* (6), 3264-3271.

26. Bingham, N.; Nisa, Q.; Gupta, P.; Young, N.; Velliou, E.; Roth, P., Biocompatibility and Physiological Thiolytic Degradability of Radically-made Thioester-functional Copolymers. *Biomacromolecules* **2022,** *23* (5), 2031-2039.

27. Bingham, N. M.; Nisa, Q. u.; Chua, S. H. L.; Fontugne, L.; Spick, M. P.; Roth, P. J., Thioester-Functional Polyacrylamides: Rapid Selective Backbone Degradation Triggers Solubility Switch Based on Aqueous Lower Critical Solution Temperature/Upper Critical Solution Temperature. *ACS Applied Polymer Materials* **2020**.

28. Bingham, N. M.; Roth, P. J., Degradable vinyl copolymers through thiocarbonyl addition–ring-opening (TARO) polymerization. *Chem. Commun.* **2019,** *55* (1), 55-58.

29. Galanopoulo, P.; Gil, N.; Gigmes, D.; Lefay, C.; Guillaneuf, Y.; Lages, M.; Nicolas, J.; Lansalot, M.; D'Agosto, F., One-Step Synthesis of Degradable Vinylic Polymer-Based Latexes via Aqueous Radical Emulsion Polymerization. *Angew. Chem. Int. Ed. Engl.* **2022,** *61* (15), e202117498.

30. Gil, N.; Caron, B.; Siri, D.; Roche, J.; Hadiouch, S.; Khedaioui, D.; Ranque, S.; Cassagne, C.; Montarnal, D.; Gigmes, D., Degradable Polystyrene via the Cleavable Comonomer Approach. *Macromolecules* **2022,** *55* (15), 6680-6694.

31. Gil, N.; Thomas, C.; Mhanna, R.; Mauriello, J.; Maury, R.; Leuschel, B.; Malval, J.-P.; Clément, J.-L.; Gigmes, D.; Lefay, C., Thionolactone as Resin Additive to Prepare (bio) degradable 3D Objects via VAT Photopolymerization. *Angew. Chem. Int. Ed.* **2021,** *134* (18), e202117700.

32. Smith, R. A.; Fu, G.; McAteer, O.; Xu, M.; Gutekunst, W. R., Radical Approach to Thioester-Containing Polymers. *J. Am. Chem. Soc.* **2019,** *141* (4), 1446-1451.

33. Spick, M. P.; Bingham, N. M.; Li, Y.; de Jesus, J.; Costa, C.; Bailey, M. J.; Roth, P. J., Fully Degradable Thioester-Functional Homo- and Alternating Copolymers Prepared through Thiocarbonyl Addition–Ring-Opening RAFT Radical Polymerization. *Macromolecules* **2020,** *53* (2), 539-547.

34. Lages, M.; Gil, N.; Galanopoulo, P.; Mougin, J.; Lefay, C.; Guillaneuf, Y.; Lansalot, M.; D'Agosto, F.; Nicolas, J., Degradable Vinyl Copolymer Nanoparticles/Latexes by Aqueous Nitroxide-Mediated Polymerization-Induced Self-Assembly. *Macromolecules* **2022,** *55* (21), 9790-9801.

35. un Nisa, Q.; Theobald, W.; Hepburn, K. S.; Riddlestone, I.; Bingham, N. M.; Kopeć, M.; Roth, P. J., Degradable Linear and Bottlebrush Thioester-Functional Copolymers through Atom-Transfer Radical Ring-Opening Copolymerization of a Thionolactone. *Macromolecules* **2022,** *55* (17), 7392-7400.

36. Galanopoulo, P.; Gil, N.; Gigmes, D.; Lefay, C.; Guillaneuf, Y.; Lages, M.; Nicolas, J.; D'Agosto, F.; Lansalot, M., RAFT-Mediated Emulsion Polymerization-Induced Self-Assembly for the Synthesis of Core-Degradable Waterborne Particles. *Angew. Chem. Int. Ed.* **2023**, e202302093.

37. Lages, M.; Pesenti, T.; Zhu, C.; Le, D.; Mougin, J.; Guillaneuf, Y.; Nicolas, J., Degradable polyisoprene by radical ring-opening polymerization and application to polymer prodrug nanoparticles. *Chem. Sci.* **2023,** *14*, 3311-3325.

38. Lages, M.; Nicolas, J., In situ encapsulation of biologically active ingredients into polymer particles by polymerization in dispersed media. *Prog. Polym. Sci.* **2023,** *137*, 101637.

39. Aksakal, S.; Aksakal, R.; Becer, C. R., Thioester Functional Polymers. In *Sulfur-Containing Polymers*, 2021; pp 235-263.

40. Nicolas, J.; Charleux, B.; Guerret, O.; Magnet, S., Nitroxide-Mediated Controlled Free-Radical Emulsion Polymerization of Styrene and n-Butyl Acrylate with a Water-Soluble Alkoxyamine as Initiator. *Angew. Chem. Int. Ed.* **2004,** *43* (45), 6186-6189.

41. Lovell, P. A.; Schork, F. J., Fundamentals of Emulsion Polymerization. *Biomacromolecules* **2020,** *21* (11), 4396-4441.

42. Delaittre, G.; Nicolas, J.; Lefay, C.; Save, M.; Charleux, B., Surfactant-free synthesis of amphiphilic diblock copolymer nanoparticles via nitroxide-mediated emulsion polymerization. *Chem. Commun.* **2005,** (5), 614-616.

43. Farcet, C.; Belleney, J.; Charleux, B.; Pirri, R., Structural Characterization of Nitroxide-Terminated Poly(n-butyl acrylate) Prepared in Bulk and Miniemulsion Polymerizations. *Macromolecules* **2002,** *35* (13), 4912-4918.